Plasmon delocalization onset in finite sized nanostructures

Arash Farhang[1,2] and Olivier J. F. Martin[1,3]

[1]Nanophotonics and Metrology Laboratory, Swiss Federal Institute of Technology Lausanne EPFL-STI-NAM, Station 11, CH-1015 Lausanne, Switzerland
[2]arash.farhang@epfl.ch
[3]olivier.martin@epfl.ch

Abstract: The transition from localized to delocalized plasmons (i.e. the transition from a situation where the decay length of a travelling surface plasma wave is greater than its propagation distance to a situation where it is smaller) and hence the onset of plasmon delocalization is studied in a single 2D silver nanoparticle of increasing length. A fourier analysis in the near-field of the nanoparticle is used as the main tool for analysis. This method, along with far-field scattering spectra simulations and the near-field profile directly above and along the length of the nanoparticle are used to investigate and clearly show the transition from localized to delocalized modes. In particular, it is found that for a finite sized rectangular nanoparticle, both the emerging odd and even delocalized modes are nothing but a superposition of many standing wave plasmon modes. As a consequence, even very short metal films can support delocalized plasmons that bounce back and forth along the film.

OCIS codes: (250.5403) Plasmonics; (240.6680) Surface plasmons.

References and links

1. T. Rindzevicius, Y. Alaverdyan, A. Dahlin, F. Höök, D. S. Sutherland, and M. Käll, "Plasmonic sensing characteristics of single nanometric holes," Nano Lett. **5**(11), 2335–2339 (2005).
2. L. J. Sherry, R. Jin, C. A. Mirkin, G. C. Schatz, and R. P. Van Duyne, "Localized surface plasmon resonance spectroscopy of single silver triangular nanoprisms," Nano Lett. **6**(9), 2060–2065 (2006).
3. J. N. Anker, W. P. Hall, O. Lyandres, N. C. Shah, J. Zhao, and R. P. Van Duyne, "Biosensing with plasmonic nanosensors," Nat. Mater. **7**(6), 442–453 (2008).
4. A. Unger, U. Rietzler, R. Berger, and M. Kreiter, "Sensitivity of crescent-shaped metal nanoparticles to attachment of dielectric colloids," Nano Lett. **9**(6), 2311–2315 (2009).
5. W. Zhang, L. Huang, C. Santschi, and O. J. F. Martin, "Trapping and sensing 10 nm metal nanoparticles using plasmonic dipole antennas," Nano Lett. **10**(3), 1006–1011 (2010).
6. L. R. Hirsch, R. J. Stafford, J. A. Bankson, S. R. Sershen, B. Rivera, R. E. Price, J. D. Hazle, N. J. Halas, and J. L. West, "Nanoshell-mediated near-infrared thermal therapy of tumors under magnetic resonance guidance," Proc. Natl. Acad. Sci. U.S.A. **100**(23), 13549–13554 (2003).
7. D. P. O'Neal, L. R. Hirsch, N. J. Halas, J. D. Payne, and J. L. West, "Photo-thermal tumor ablation in mice using near infrared-absorbing nanoparticles," Cancer Lett. **209**(2), 171–176 (2004).
8. J. Chen, D. Wang, J. Xi, L. Au, A. Siekkinen, A. Warsen, Z.-Y. Li, H. Zhang, Y. Xia, and X. Li, "Immuno gold nanocages with tailored optical properties for targeted photothermal destruction of cancer cells," Nano Lett. **7**(5), 1318–1322 (2007).
9. A. M. Gobin, M. H. Lee, N. J. Halas, W. D. James, R. A. Drezek, and J. L. West, "Near-infrared resonant nanoshells for combined optical imaging and photothermal cancer therapy," Nano Lett. **7**(7), 1929–1934 (2007).
10. J. Homola, S. S. Yee, and G. Gauglitz, "Surface plasmon resonance sensors: review," Sens. Actuators B Chem. **54**(1-2), 3–15 (1999).
11. D. K. Gramotnev, and S. I. Bozhevolnyi, "Plasmonics beyond the diffraction limit," Nat. Photonics **4**(2), 83–91 (2010).
12. P. Berini, "Plasmon polariton modes guided by a metal film of finite width," Opt. Lett. **24**(15), 1011–1013 (1999).
13. P. Berini, R. Charbonneau, and N. Lahoud, "Long-range surface plasmons on ultrathin membranes," Nano Lett. **7**(5), 1376–1380 (2007).
14. A. Degiron, S.-Y. Cho, C. Harrison, N. M. Jokerst, C. Dellagiacoma, O. J. F. Martin, and D. R. Smith, "Experimental comparison between conventional and hybrid long-range surface plasmon waveguide bends," Phys. Rev. A **77**(2), 021804 (2008).

#145562 - $15.00 USD Received 7 Apr 2011; revised 12 May 2011; accepted 15 May 2011; published 26 May 2011

15. G. Colas des Francs, J. Grandidier, S. Massenot, A. Bouhelier, J.-C. Weeber, and A. Dereux, "Integrated plasmonic waveguides: a mode solver based on density of states formulation," Phys. Rev. B **80**(11), 115419 (2009).
16. A. Degiron, S.-Y. Cho, T. Tyler, N. M. Jokerst, and D. R. Smith, "Directional coupling between dielectric and long-range plasmon waveguides," N. J. Phys. **11**(1), 015002 (2009).
17. M. I. Stockman, S. V. Faleev, and D. J. Bergman, "Localization versus delocalization of surface plasmons in nanosystems: can one state have both characteristics?" Phys. Rev. Lett. **87**(16), 167401 (2001).
18. S. Balci, A. Kocabas, C. Kocabas, and A. Aydinli, "Localization of surface plasmon polaritons in hexagonal arrays of Moire cavities," Appl. Phys. Lett. **98**(3), 031101–031103 (2011).
19. G. Lévêque, and O. J. F. Martin, "Optical interactions in a plasmonic particle coupled to a metallic film," Opt. Express **14**(21), 9971–9981 (2006).
20. A. Christ, G. Lévêque, O. J. F. Martin, T. Zentgraf, J. Kuhl, C. Bauer, H. Giessen, and S. G. Tikhodeev, "Near-field-induced tunability of surface plasmon polaritons in composite metallic nanostructures," J. Microsc. **229**(Pt 2), 344–353 (2008).
21. B. Luk'yanchuk, N. I. Zheludev, S. A. Maier, N. J. Halas, P. Nordlander, H. Giessen, and C. T. Chong, "The Fano resonance in plasmonic nanostructures and metamaterials," Nat. Mater. **9**(9), 707–715 (2010).
22. P. B. Johnson, and R. W. Christy, "Optical constants of the noble metals," Phys. Rev. B **6**(12), 4370–4379 (1972).
23. W. Lukosz, and M. Meier, "Lifetimes and radiation patterns of luminescent centers close to a thin metal film," Opt. Lett. **6**(5), 251–253 (1981).
24. M. Paulus, and O. J. F. Martin, "Green's tensor technique for scattering in two-dimensional stratified media," Phys. Rev. E Stat. Nonlin. Soft Matter Phys. **63**, 066615 (2001).
25. R. H. Ritchie, "Plasma losses by fast electrons in thin films," Phys. Rev. **106**(5), 874–881 (1957).
26. D. Sarid, "Long-range surface-plasma waves on very thin metal films," Phys. Rev. Lett. **47**(26), 1927–1930 (1981).
27. S. A. Maier, *Plasmonics: Fundamentals and Applications* (Spinger-Verlag, 2007).
28. J. Nelayah, M. Kociak, O. Stéphan, N. Geuquet, L. Henrard, F. J. García de Abajo, I. Pastoriza-Santos, L. M. Liz-Marzán, and C. Colliex, "Two-dimensional quasistatic stationary short range surface plasmons in flat nanoprisms," Nano Lett. **10**(3), 902–907 (2010).

1. Introduction

Plasmonics, the bridge between the best of optics and electronics, is based on resonant electron plasma oscillations in metallic nanostructures. Formally there are two types of plasmon resonances, localized plasmons and delocalized plasmons. The former, confined around nanoparticles, nanoantennas, and various other compact nanostructures, allows for very high near-field enhancements at optical frequencies due to high localizations of the scattered field and has been shown useful in applications ranging from trapping and sensing [1–5] to cancer treatment [6–9]. The latter, based on the free propagation of surface waves at an extended metal dielectric interface, has played a major role in the development of surface plasmon based biosensors [10] and shows great promise in the development of ultra-fast and compact optical circuitry [11–16].

Traditionally, plasmonic systems studied support either localized or delocalized resonances. Small finite structures are found to support localized modes and infinite structures are found to support delocalized modes. Systems containing both small finite and infinite structures, such as ordered and disordered metal films [17,18] as well as metal nanoparticle and film systems [19] are found to exhibit both resonances, which can lead to Fano interferences [20,21]. The response of intermediately sized structures and hence the transition from localized to delocalized states, however, has yet to be studied. In this paper, we investigate the response of a 2D silver nanoparticle of fixed thickness and increasing length, and in doing so demonstrate the onset of plasmon delocalization.

In Section 2, we discuss the geometry investigated and give details on the analysis methods. Particularly we point out intrinsic limitations of the analysis method used in order to aid in the understanding of the obtained results. Subsequently in Section 3, we show how to excite both even and odd delocalized/propagating modes, thus providing all the necessary tools for the study at hand. In Section 4, we demonstrate and discuss the onset of plasmon delocalization for even and odd propagating modes and in Section 5, provide a brief summary.

#145562 - $15.00 USD Received 7 Apr 2011; revised 12 May 2011; accepted 15 May 2011; published 26 May 2011

2. Geometry and analysis techniques

The geometry investigated is a 2D 40nm thick silver nanoparticle of variable length L in freespace (Fig. 1). A 2D geometry was chosen since effects along the 3rd dimension are invariant. We use the dielectric data of silver measured by Johnson and Christy [22]. As shown, an electric dipole source is used because it will allow for the excitation of localized modes and also for the launching of delocalized/propagating modes without the use of gratings or methods such as prism coupling [23]. We start with a length L = 50nm and with each successive step gradually increase the nanoparticle length, thus allowing us to observe the transition from localized to delocalized modes.

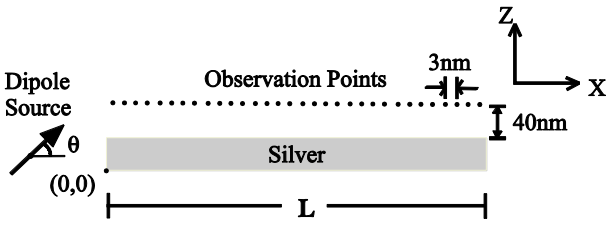

Fig. 1. A silver nanoparticle of length L excited by an electric dipole source. The corner of the nanoparticle marks the origin. The dipole source is placed at a position of (–100nm, 20nm).

The simulation method carried out for this study is based on the Green's Tensor formalism in 2D [24]. We locate the resonance position of the localized modes by calculating the integrated scattering spectra in the far-field around the particle. Analysis of the delocalized/propagating modes of the system is accomplished by performing a Fourier analysis of the scattered field 40nm above the surface of the nanoparticle. For this we sample the scattered electric field at numerous observation points with a 3nm spacing (Fig. 1). We chose only a 40nm distance above the nanoparticle in order to probe the evanescent tail of the surface plasmon. For analysis, we apply a hamming window to the data, zero pad it to give a total array length of 20,000, and then perform an FFT and an FFT-shift to obtain the k-vector vs. frequency response of the system. Unlike the analytically obtained dispersion of an infinite silver film, where the imaginary component of the k-vector represents loss, the imaginary component of the k-vector obtained through the Fourier analysis resolves phase. Since the phase is of no relevance to our study, all k-vector vs. frequency plots present only the k-vector magnitude. Note, in all 3D plots, results have been normalized prior to plotting.

We have chosen a 3nm spacing of the observation points in order to ensure that even very large propagation vectors are well resolved. In addition, zero padding is applied to give a total array length of 20,000; this is to ensure uniform resolution in k-space for every particle length L investigated. Padding with many zeros also has a very nice effect, as it provides for interpolation of the data in k-space, which is especially desirable for nanoparticles of shorter lengths. This is because the total number of sampling points is inherently low for small L and thus the resulting resolution in k-space, if zero padding is not applied, will be very coarse. Additionally for small L, the Fourier analysis method poses a second intrinsic limitation. Theoretically, the use of a Fourier transform can provide exact k-vector information, however, when using a discrete Fourier transform, such as an FFT, only a finite range of data can be taken. This of course is problematic because in order to exactly represent any sort of infinite periodic function one needs an infinite range of data. The smaller the sampling range, the higher the uncertainty of the resulting k-vector. Specifically in this study, we see that as the length L and thus the sampling range increase, the amount of spectral broadening in k-space decrease.

#145562 - $15.00 USD Received 7 Apr 2011; revised 12 May 2011; accepted 15 May 2011; published 26 May 2011

3. Mode excitation

For a metallic film of thickness $2a$ in freespace, there exists two propagating modes, an even/short range and an odd/long range mode [25,26]. The wave vector k for odd and even modes is given by Eq. (1) and (2) respectively, where $\varepsilon_m = \varepsilon_r + i\varepsilon_i$ is the complex dielectric permittivity of the metal, $k_{z,m}$ and $k_{z,f}$ given by Eq. (3) and (4) are the z-components of the wave vector in the metal and freespace respectively, and k_0 is the total freespace wave vector [27].

$$\tanh k_{z,m}a = -\frac{k_{z,f}\varepsilon_m}{k_{z,m}}, \tag{1}$$

$$\tanh k_{z,m}a = -\frac{k_{z,m}}{k_{z,f}\varepsilon_m}, \tag{2}$$

$$k_{z,m} = \sqrt{k^2 - k_0^2\varepsilon_m}, \tag{3}$$

$$k_{z,f} = \sqrt{k^2 - k_0^2}. \tag{4}$$

For a 40nm thick film, these equations yield the following real and imaginary components of the k-vector for the odd and even propagating modes (Fig. 2). The real components give the k-vector of the excited mode, while the imaginary components give ohmic propagation losses [27].

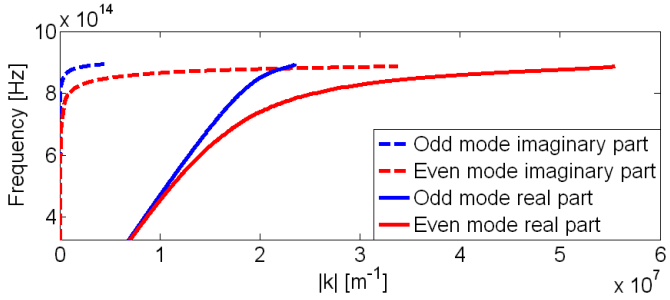

Fig. 2. Analytically obtained dispersion of a 40nm thick, infinite silver film, showing the real and imaginary parts of the k-vector for even and odd propagating modes.

We wish for this study to excite both even and odd modes separately. As shown in Fig. 1, the dipole orientation is defined by the angle θ. We have two extreme cases for the dipole orientation, θ = 0° and θ = 90°. In Fig. 3 we show the effect of each orientation on a particle of infinite length and plot the resulting electric field distributions. For θ = 0° the horizontal dipole will induce alternating horizontal dipoles in the metal, which results in the same alternating positive/negative charge distribution at both the top and bottom surfaces of the metal. For θ = 90° the vertical dipole will induce alternating vertical dipoles in the metal, resulting in opposing positive negative charge distributions at the top and bottom surfaces of the metal. It can be seen from the charge and the resulting electric field distributions, that for θ = 0° the even propagating mode should be excited and that for θ = 90° the odd propagating mode should be excited. We can also see that for very small L and θ = 0°, the excited localized mode will just be a dipolar mode oscillating along the length of the nanoparticle. For θ = 90°, however, the localized dipolar mode will be along the thickness of the nanoparticle and thus its resonance frequency should not change with L. Most interesting, however, is the middle ground where L is neither very small nor effectively infinite. We can speculate what may happen for intermediate L by looking at the charge distribution and field lines of the

#145562 - $15.00 USD Received 7 Apr 2011; revised 12 May 2011; accepted 15 May 2011; published 26 May 2011

infinitely long particle (Fig. 3) up to a distance of L from the start of the particle and ignoring everything after that point. The termination of the metallic particle at a length L will simply result in a reflection at the interface. We will revisit this interpretation in Section 4 where we present in depth the onset of plasmon delocalization.

For the geometry being studied, we expect the existence of even and odd propagating modes for a sufficiently large length L. Due to the exponentially growing computational time with increasing particle length L, we limit the maximum simulation length to L = 20μm, which corresponds to several surface plasmon propagation lengths. The movie corresponding to Fig. 4 shows the excitation of even and odd modes for L = 20μm as the dipole is rotated from θ = 0° to θ = 90°. As expected, for a θ = 0° only the even mode is excited, while for θ = 90° only the odd mode is excited. We see for θ = 45° that both even and odd modes are excited. Note that in the Fourier analysis we sample the z-component of the scattered light, hence the air light line is strongest at θ = 90° and virtually non-existent at θ = 0°.

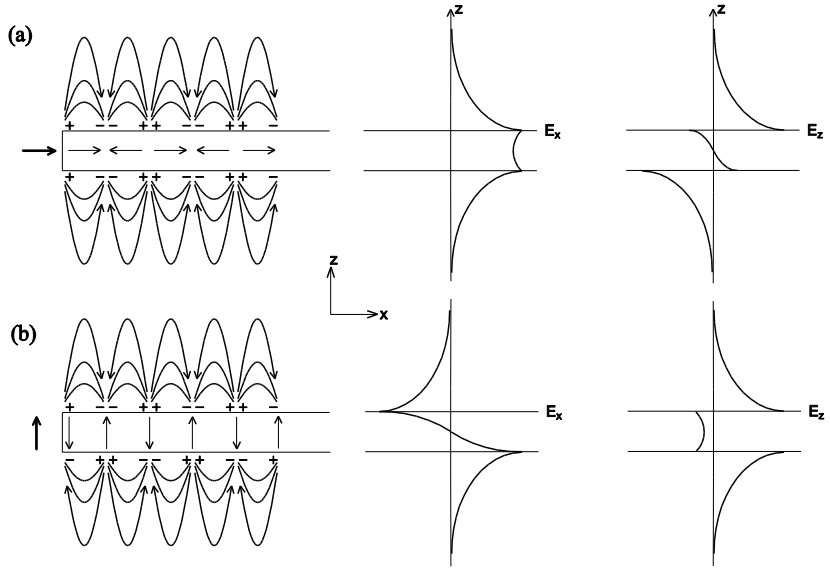

Fig. 3. Effect of horizontal and vertical dipole sources on an infinitely long metallic nanoparticle and the resulting electric field distributions. (a) A horizontal dipole excites the even propagating mode, while (b) a vertical dipole excites the odd mode.

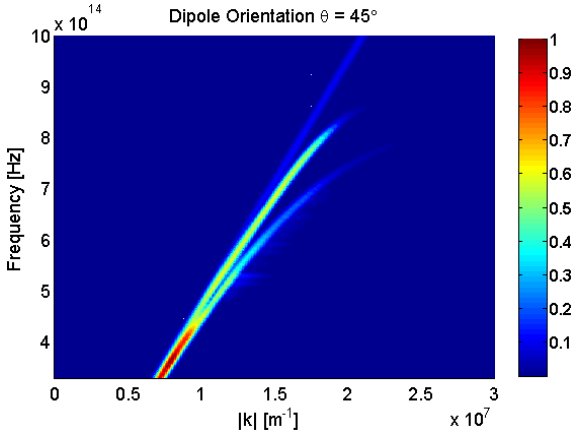

Fig. 4. Dispersion relation computed for an L = 20μm particle, excited by a dipole source rotating from 0 to 90°. Only the even mode is excited for θ = 0° and only the odd mode for θ = 90°. (Media 1)

#145562 - $15.00 USD Received 7 Apr 2011; revised 12 May 2011; accepted 15 May 2011; published 26 May 2011

We expect from Fig. 2 to see in Fig. 4 the extension of the even and odd mode k-vectors to $5.5\text{x}10^7\text{m}^{-1}$ and $2.4\text{x}10^7\text{m}^{-1}$ respectively; however, due to propagation losses this is not the case. In addition, we expect that some of the propagating plasmon will reflect back, thus resulting in negative k-vector values. In order to investigate this and the extent of propagation losses, we plot in Fig. 5 the results for a dipole angle of $\theta = 45°$ on a base 10 logarithmic scale. A logarithmic scale was chosen to show the extent of the k-vector even with high losses that occur close to the limiting surface plasmon frequencies and also to better display any backwards propagation due to reflections at the end of the particle. It can be seen that above approximately 870THz, losses are very high and thus completely restrict mode propagation. In addition, it can be seen for lower frequencies (i.e. low loss regions) that the propagating plasmon sees the end of the nanoparticle and reflects back, resulting in negative k-vector values.

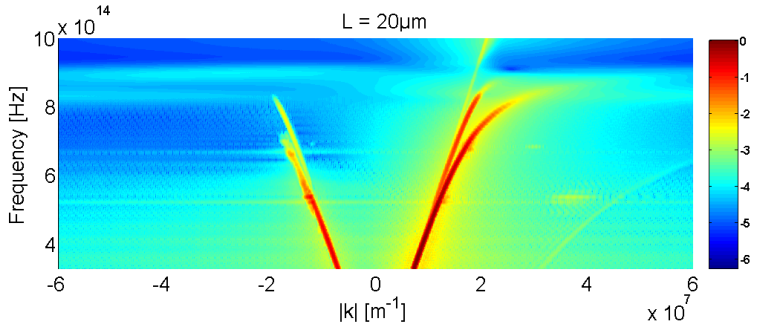

Fig. 5. Excitation of even and odd propagating modes for a particle of length L = 20μm by a θ = 45° dipole source plotted on a base 10 logarithmic scale. Notice negative k values showing the back propagation of the surface plasmon waves.

4. Onset of plasmon delocalization

4.1 Even propagating mode

Excitation of the even propagating mode in an elongated nanoparticle, as seen in Sec. 3, requires the use of a dipole source orientation of $\theta = 0°$. For small L, one will excite a localized dipolar mode across the length of the particle, Fig. 3(a); hence, we expect a transition from this dipolar mode to the propagating mode at the onset of plasmon delocalization. Revisiting the proposed interpretation for nanoparticles of intermediate length presented in the second paragraph of the previous section, we can see for a dipole angle $\theta = 0°$, as L is increased we will go from a single dipole across the length of the nanoparticle to two opposing dipoles then three opposing dipoles and so on. These alternating dipoles result in alternating surface charges, which of course are exactly what one has for a propagating plasmon mode. We thus expect to see the propagation of plasmons once the length has increased sufficiently to support multiple alternating dipoles. We of course wish to study this using the Fourier analysis method presented in Section 2, however, for very short particle lengths, resulting spectral broadening yields indiscernible Fourier analysis results. For this reason, we only concentrate on far-field scattering spectra for small L. Specifically, we begin by looking at the scattering spectra for ten nanoparticles of lengths L = 50-500nm (Fig. 6).

For L = 50nm a single dipolar mode is observed at about 830THz. For L = 100nm the mode redshifts. For L = 150nm the mode redshifts further and a second higher order mode appears at about 820THz. As L increases these two modes continue to redshift and then for L = 250nm a third higher order mode appears at around 830THz. It can be seen in each subsequent panel that as L increases the modes continue to shift and additional higher order modes continually emerge.

#145562 - $15.00 USD Received 7 Apr 2011; revised 12 May 2011; accepted 15 May 2011; published 26 May 2011

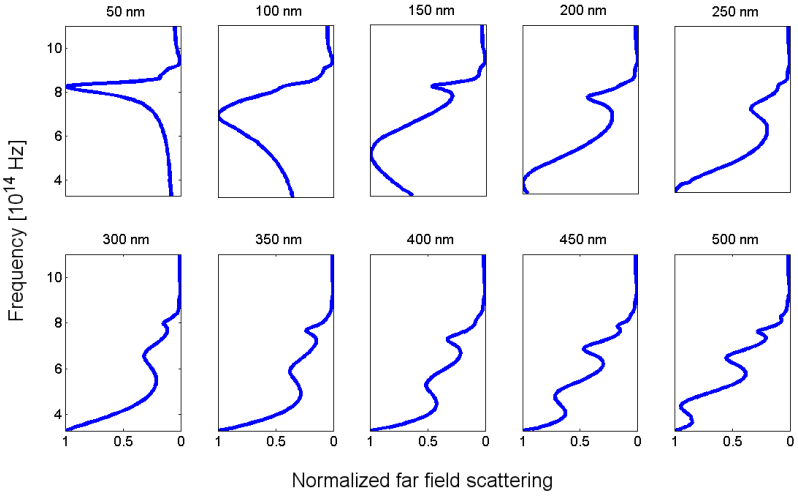

Fig. 6. Normalized scattering spectra for particles of L = 50-500nm, excited by a θ = 0° dipole source. For successively larger lengths L, higher order modes are excited.

We now plot the data obtained through the Fourier analysis method for much longer particles of lengths 2.5 μm and 5μm, together with the scattering spectra for comparison (Fig. 7). Note we use the z-component of the scattered light in the Fourier analysis of the even mode, since it is virtually free of any freespace propagating light and thus allows for a clearer view of the plasmon modes. We see in these results the dispersion curve of the even propagating mode. Comparing the scattering spectra with the dispersion diagram, one sees numerous maxima along the dispersion curve whose spectral positions correspond exactly to those of the higher order modes. As L increases from 2.5μm to 5μm an ever greater number of these modes appear. It is obvious from this trend, that in the limit where $L \to \infty$, there will be a continuum of these higher order modes, rather than a finite number, and that the even delocalized mode is exactly this continuum. Formation of this continuum can easily be seen in the movie linked to Fig. 4 for a dipole orientation θ = 0°. Here for L = 20μm we are virtually unable to distinguish one mode from another.

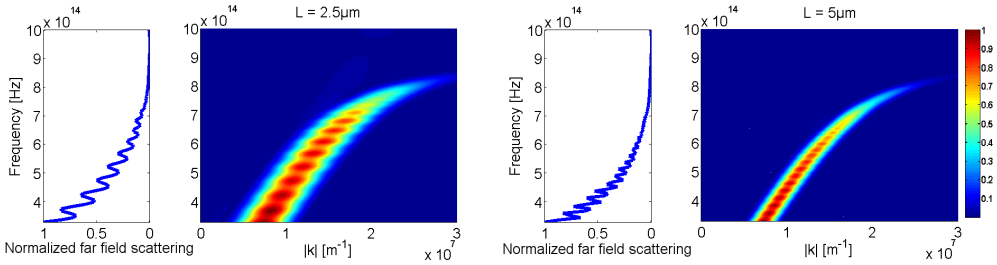

Fig. 7. Fourier analysis and scattering spectra results for L = 2.5 and 5μm. We excite the even propagating surface plasmon mode with a horizontally oriented dipole source. As can be seen, for a finite particle length, this mode is nothing more than the superposition of many higher order modes.

We provide further insight into the nature of this transition by plotting the field distribution along the line of observation points shown in Fig. 1, for L = 5μm and for a much shorter L = 500nm (Fig. 8). We see for L = 5μm at frequencies approximately below 700THz, standing wave patterns, hence the higher order modes seen in the Fourier analysis results are just standing wave surface plasmons formed by the interference of the forward and back propagating waves, Fig. 8 right panel. Actually, a similar effect has been observed by J. Nelayah et al. in plasmonic nanoprisms [28]. In fact, for any given frequency, the spacing between two intensity maxima is exactly half the surface plasmon wavelength, the surface

#145562 - $15.00 USD Received 7 Apr 2011; revised 12 May 2011; accepted 15 May 2011; published 26 May 2011

plasmon wavelength being that taken from the k-vector vs. frequency plots of Fig. 7. Above frequencies of approximately 700THz, where the peaks of higher order modes are no longer apparent (Fig. 7), we see only the exponential decay of highly damped propagating plasmons (Fig. 8), due to the fact that losses have become increasing significant (Fig. 2). As predicted, the presence of even just a few alternating dipoles results in the propagation of plasmon waves. This is evident in the standing wave patterns seen for a nanoparticle of just L = 500nm, Fig. 8 left panel. More surprising, however, is that even in the case of just two alternating dipoles, a standing wave behavior is still present. This can be seen by comparing the scattering of L = 500nm in Fig. 6 with the field distribution in Fig. 8. The peak for the second mode (two opposing dipoles) falls at about 430THz. The standing wave pattern at this frequency in Fig. 8 corresponds exactly to this, as it is composed of one central peak and two others at the nanoparticles ends. As one expects, for this short length, standing wave patterns are indeed present up to much higher frequencies (above 800THz) than for L = 5μm, due to the fact that the delocalized mode has a much shorter distance to propagate before reaching the end and reflecting back. Let us finally note that the charge distribution of the modes in Fig. 8 perfectly reproduces that shown in Fig. 3(a).

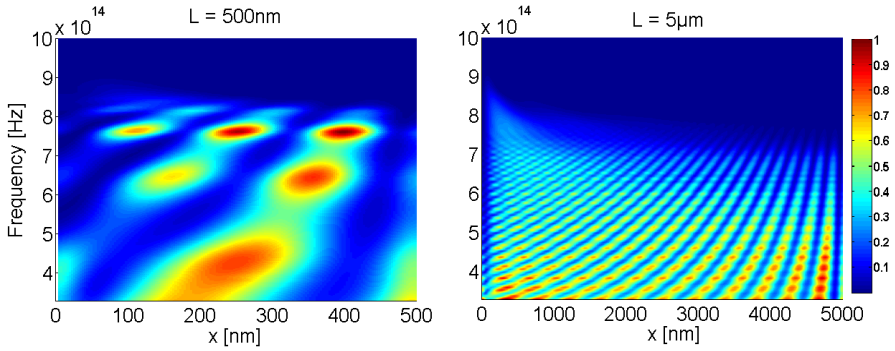

Fig. 8. Field distribution along the line of observation points 40nm above L = 500nm and 5μm long nanoparticles. For L = 5μm, standing wave patterns are clearly seen below approximately 700THz due to interference between forward and back propagating plasmons. Only the evanescent decay of the surface plasmon is seen at higher frequencies. Even down to a very short length of 500nm, the standing wave pattern is still present.

4.2 Odd propagating mode

Excitation of the odd propagating mode in an elongated nanoparticle, as seen in Sec. 3, requires the use of a dipole source orientation of θ = 90°. For any length L, a dipolar mode will be excited along the 40nm height. For very long particles, we should of course see this mode be concentrated primarily at the end of the nanoparticle closest to the dipole source. Additionally, from the scattering spectra results for L = 50nm (Fig. 6), we expect to see this dipolar resonance for L = 40nm at a frequency somewhat greater than 830THz. Furthermore, just as was the case for the even mode, here we expect to go from a single vertical dipole to two opposing vertical dipoles to three and so on as the particle length is increased. In the same way as before these result in alternating surface charges and we again should see propagation of plasmons once the length has become sufficiently large. We plot in Fig. 9 Fourier analysis results for particles of lengths 1μm and 5μm. For L = 1μm we clearly see what we assume to be the vertical dipole resonance at around 880THz. We see an additional resonance at around 820THz. For L = 5μm we see the resonance centered at 820THz spectrally broaden and the dipolar resonance at approximately 880THz diminishing. Since a Fourier analysis is performed over the entire particle length and since the dipolar mode is assumed to exist primarily at the left end of the nanoparticle, it is only natural that as L increases that the localized mode will seemingly diminish.

#145562 - $15.00 USD Received 7 Apr 2011; revised 12 May 2011; accepted 15 May 2011; published 26 May 2011

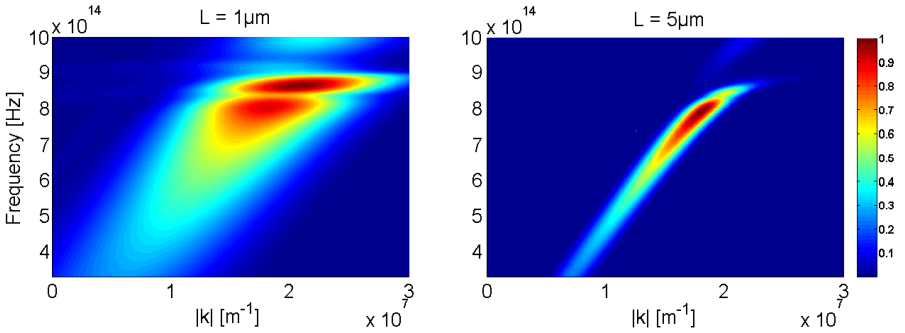

Fig. 9. Fourier analysis results for L = 1 and 5μm. We excite the odd propagating surface plasmon mode with a vertically oriented dipole source and at the same time excite a localized dipolar resonance along the 40nm height of the particle at approximately 880THz. As can be seen, for L = 1μm the propagating mode is mainly confined to approximately 820THz where the propagating plasmon is most efficiently excited and as the particle length is increased to 5μm it is found to spectrally broaden.

In order to gain further insight into these phenomena, we plot as was done in Fig. 8, the field distribution above the particle for lengths 1μm and 5μm (Fig. 10). We see clearly in both plots the localized mode at around 880THz, mainly towards the left end of the nanoparticle, closest to the excitation source. This fact confirms why the localized resonance seemingly diminishes in the Fourier analysis results of Fig. 9 as L increases from 1μm to 5μm. We see for L = 1μm a standing wave pattern at about 820THz, indicating the presence of a propagating mode. In the field distribution for L = 5μm, where this mode has broadened, the standing wave pattern becomes visible down to lower frequencies as well, though it is still most prevalent at 820THz. Additional transfer matrix simulations for a 40nm thick infinite silver film in freespace indicate that it is around 820THz where the odd/long range mode is most efficiently excited (not shown here). Hence for shorter lengths where the propagating wave undergoes many reflections at the ends of the particle, the standing wave formed at this frequency will dominate, even though propagating plasmons at lower frequencies are still excited. For L = 20μm as seen in the last panel of the movie linked to Fig. 4 (dipole orientation θ = 90°), we see the reduction of this effect and the spectral broadening of the propagating mode all the way down to 400THz. We saw in Fig. 8 a clear presence of even propagating mode for a length of just 500nm. We see in Fig. 11 that the odd propagating mode is not just present down to L = 500nm, but all the way down to L = 250nm. We again note that the charge distribution of the modes in Fig. 10 perfectly reproduces that shown in Fig. 3(b).

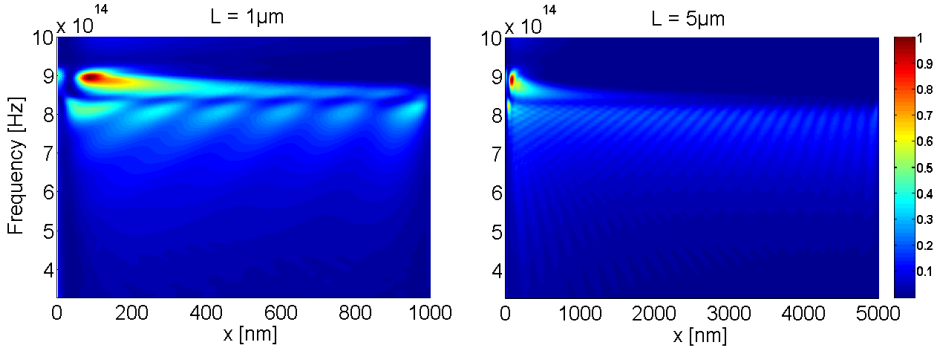

Fig. 10. Field distribution along the line of observation points 40nm above nanoparticles of L = 1 and 5μm. For both lengths, the localized dipolar resonance along the 40nm height of the particle is seen at approximately 880THz. For L = 1μm, a clear standing wave pattern, due to the odd propagating mode, is seen at about 820THz. For L = 5μm, the standing wave extends down to lower frequencies as the mode is broadened.

#145562 - $15.00 USD Received 7 Apr 2011; revised 12 May 2011; accepted 15 May 2011; published 26 May 2011

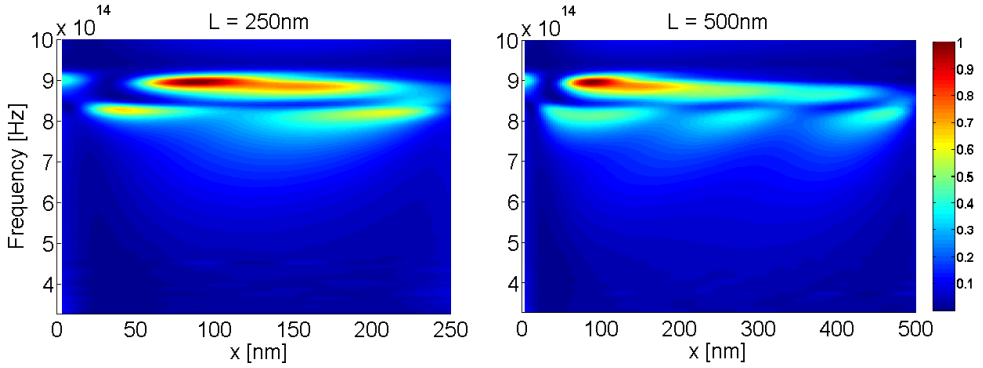

Fig. 11. Field distribution along the line of observation points 40nm above particles of lengths L = 250nm and 500nm. Even for these short lengths, the standing wave surface plasmon at around 820THz (also in Fig. 9) is still present.

5. Summary

We have studied the onset of plasmon delocalization (i.e. the transition from a situation where the decay length of a travelling surface plasma wave is greater than its propagation distance to a situation where it is smaller) both for even and odd propagating modes in a 2D silver nanoparticle of increasing length L. A Fourier analysis performed 40nm above and along the length of the particle showed clear excitation of both propagating modes for the largest length L = 20μm studied. Using this method, together with far-field scattering spectra results, and the field distribution profile 40nm above the particle, we showed clearly the transition from localized to delocalized modes as the particle length was increased. In particular, we showed for finite lengths that the even propagating mode is nothing but a superposition of numerous high order modes, these modes being just standing wave plasmons. The odd mode was also shown to be the superposition of many standing wave modes. Due to its long range nature, however, it was found to be predominantly a single standing wave at the frequency of most efficient excitation (approximately 820THz) and to broaden to the usual continuum of the odd mode as the particle length was increased.

Acknowledgment

Funding from the State Secretariat for Education and Research SER within the Indo Swiss Joint Research Programme is gratefully acknowledged.

#145562 - $15.00 USD Received 7 Apr 2011; revised 12 May 2011; accepted 15 May 2011; published 26 May 2011